Since January 2020 Elsevier has created a COVID-19 resource centre with free information in English and Mandarin on the novel coronavirus COVID-19. The COVID-19 resource centre is hosted on Elsevier Connect, the company's public news and information website.

Available online at www.sciencedirect.com
SCIENCE DIRECT
Virology 350 (2006) 1 – 14
VIROLOGY
www.elsevier.com/locate/yviro

Visualization of the African swine fever virus infection in living cells by incorporation into the virus particle of green fluorescent protein-p54 membrane protein chimera

Bruno Hernaez, Jose M. Escribano, Covadonga Alonso *

Departamento de Biotecnología, INIA, Carretera de la Coruña Km 7, 28040 Madrid, Spain

Received 23 November 2005; returned to author for revision 17 December 2005; accepted 16 January 2006
Available online 21 February 2006

Abstract

Many stages of African swine fever virus infection have not yet been studied in detail. To track the behavior of African swine fever virus (ASFV) in the infected cells in real time, we produced an infectious recombinant ASFV (B54GFP-2) that expresses and incorporates into the virus particle a chimera of the p54 envelope protein fused to the enhanced green fluorescent protein (EGFP). The incorporation of the fusion protein into the virus particle was confirmed immunologically and it was determined that p54-EGFP was fully functional by confirmation that the recombinant virus made normal-sized plaques and presented similar growth curves to the wild-type virus. The tagged virus was visualized as individual fluorescent particles during the first stages of infection and allowed to visualize the infection progression in living cells through the viral life cycle by confocal microscopy. In this work, diverse potential applications of B54GFP-2 to study different aspects of ASFV infection are shown. By using this recombinant virus it was possible to determine the trajectory and speed of intracellular virus movement. Additionally, we have been able to visualize for first time the ASFV factory formation dynamics and the cytophatic effect of the virus in live infected cells. Finally, we have analyzed virus progression along the infection cycle and infected cell death as time-lapse animations.

Keywords: African swine fever virus; GFP; Fluorescent tagged virus; Viral factory; Morphogenesis

Introduction

Many aspects of the infection cycle of African swine fever virus (ASFV) remain still poorly understood. Some events of the infection such those viral proteins involved in the virus attachment, the intracellular transport to perinuclear areas of the nucleus for virus replication, as well as morphogenesis and transport events of the intracellular virus away from the factories have been biochemically defined. However, a clear understanding of these processes, how and when they occur, has been hampered by the inability to directly observe these events in infected cells.

ASFV assembly occurs in viral factories that contain high levels of viral structural proteins, viral DNA, and amorphous membranous material used to produce viral envelopes. The 170-kb genome of ASFV encodes some 150 open reading frames, and as many as 50 viral proteins are incorporated to the viral particle (Esteves et al., 1986). Approximately 35% of the mass of the virion is provided by p72, the major capsid protein, while the structural proteins p150, p37, p34 and p14, all of them derived from polyprotein p220, provides another 25% of the virion mass (Andres et al., 1997). ASFV particles assemble within cytoplasmic viral factories from endoplasmic reticulum-derived viral membranes (Andres et al., 1997, 1998; Rouiller et al., 1998) at perinuclear sites (Nunes et al., 1975) that contain fully assembled virions seen as 200-nm-diameter hexagons in cross-section, and a series of one to six-sided assembly intermediates (Rouiller et al., 1998). Morphological

Abbreviations: Ara-c, cytosine β-arabinofuranoside; ASFV, African swine fever virus; β-gal, β-galactosidase; EGFP, enhanced green fluorescent protein; ORF, open reading frame; MOI, multiplicity of infection; MW, molecular weight; wb, western blot.

* Corresponding author.
E-mail addresses: hernaez@inia.es (B. Hernaez), escriban@inia.es (J.M. Escribano), calonso@inia.es (C. Alonso).

0042-6822/$ - see front matter © 2006 Elsevier Inc. All rights reserved.
doi:10.1016/j.virol.2006.01.021

evidence indicates that viral membranes become icosahedral particles by the progressive construction of the outer capsid layer, which is composed mainly of viral protein p72 (Garcia-Escudero et al., 1998). Biochemical data also suggest that protein p72 is assembled in a time-dependent fashion into large membrane-bound complexes that may correspond to capsid-like structures (Cobbold and Wileman, 1998). Concomitantly, the core shell is formed underneath the viral envelope, and subsequently the viral DNA and nucleoproteins are packaged and condensed to form the electrondense nucleoid (Andres et al., 1997, 2002; Brookes et al., 1998). Intracellular mature virions made at the assembly sites are infectious (Andres et al., 2001). A fraction of them, however are transported by microtubule-mediated transport (Alonso et al., 2001; de Matos and Carvalho, 1993) to the plasma membrane, where they are released by budding (Breese and Pan, 1978) to give rise to the infectious extracellular enveloped virions.

Because of the high viscosity of the cytoplasm, movement of ASFV particles by diffusion is likely to be very limited (for review see (Luby-Phelps, 2000). Some viruses overcome this obstacle by hijacking cytoplasmic motors to utilize the cellular cytoskeleton as a roadway. For instance, herpes simplex virus HSV-1, adenovirus, ASFV and rabies virus are thought to use dynein motors to travel along microtubule network for intracellular transport (Alonso et al., 2001; Raux et al., 2000; Sodeik et al., 1997; Suomalainen et al., 1999). ASFV interacts with the dynein motor complex through the structural virus protein p54 (Alonso et al., 2001). To further characterize the intracellular trafficking of some of these viruses, several fluorescence-based methods have been developed allowing the detection and characterization of intracellular complexes of viral origin. Importantly, several of these labeling methods allow the visualization of individual virions in living cells (Smith and Enquist, 2002). These studies suggest that the intracellular trafficking of these viruses is a highly ordered process using cellular motor pathways. Similarly, with tagged viruses it would be possible to visualize virus morphogenesis and cytopathic effects produced in the cells as infection progresses.

In this report, we describe the construction of an ASF recombinant virus, in which we have exchanged the single copy of the p54 open reading frame in the ASFV genome, gene *E183L* (Rodriguez et al., 1994) with a chimeric gene encoding p54-EGFP. Interestingly, this virus is fully viable and exhibits growth kinetics similar to those of its parental virus. Moreover, p54-EGFP is incorporated into the virus particle with the same efficiency as p54. The presence of p54-EGFP in the virion results in fluorescent particles which are readily visualized with a fluorescence microscope, allowing visualization of p54-EGFP within live cells. As a consequence of such sensitive detection of p54-EGFP throughout infection, we have been able to use time lapse confocal microscopy to monitor the trafficking of p54-EGFP within individual cells. We present those results as subsequent images and time lapse animations. Thus, we have generated a reagent which will enable the visualization of several aspects of ASFV infection in live cells, including virus entry, assembly, trafficking and apoptotic cell death.

Results

Construction of a recombinant ASFV expressing p54-EGFP fusion protein

The main goal of the molecular manipulations described below was to generate a tagged ASF virion that allowed us monitoring the infection in living cells. We selected the ASFV envelope protein p54, encoded by the essential *E183L* gene (Rodriguez et al., 1994), to drive the EGFP incorporation into the virus envelope. Then, we replaced the protein p54 in the virus particle by p54-EGFP fusion chimera in two steps. First, we introduced in the *TK* gene of the virus the sequence encoding the fusion protein p54-EGFP under the control of p54 promoter (Fig. 1a). Recombinant virus plaques exhibiting green fluorescence were picked and individual recombinant viruses were further plaque purified by limiting dilution and screened by PCR and Southern blot to confirm the presence of the p54-EGFP coding sequence in the TK locus, as expected (Fig. 1b). The recombinant virus obtained was designated as B54GFP-1 and used to infect cells to visualize the fluorescence properties of individual virus clones (Figs. 1c and d). Moreover, the use of EGFP as marker gene allowed a faster detection of recombinant viral plaques when compared to wild-type virus (data not shown). EGFP fusion to a specific protein often modifies its inherent properties, so we first determined whether the addition of EGFP to the C- terminus of p54 could affect the usual subcellular distribution of this protein. Then, Vero cells were infected with B54GFP-1 or wild-type virus (BA71V) and subcellular distributions of p54-EGFP and p54 were examined by conventional immunofluorescence microscopy (Figs. 1e–j). No differences were observed when compared, demonstrating that typical perinuclear accumulation described for p54 in ASFV infection was not altered by the GFP fusion.

p54 is an essential protein and then to study p54-EGFP functionality in the virus morphogenesis and to increase the number of copies of the tagged protein in the virions, the wild-type *E183L* gene was interrupted by insertion of the β-galactosidase coding sequence. This second step in recombinant virus generation was performed by homologous recombination with vector pΔp54 which contains the β-galactosidase coding sequence under the control of p72 promoter and flanqued by 424 pb and 888 pb from p54 *E183L* right and left extremes, respectively. Resulting recombinant virus plaques exhibiting β-gal activity were picked and analyzed by PCR as well as Southern blot to confirm the interruption of gene *E183L* in the genome of ASFV (Fig. 1b). After isolation by several rounds of plaque purification, all virus plaques exhibited both GFP and β-galactosidase activities. The double recombinant virus finally obtained was designated B54GFP-2 and when used to infect cells, no trace of the wild-type p54 protein could be detected by Western blot in cell extracts obtained at different times of infection using a specific anti-p54 serum (Fig. 3a).

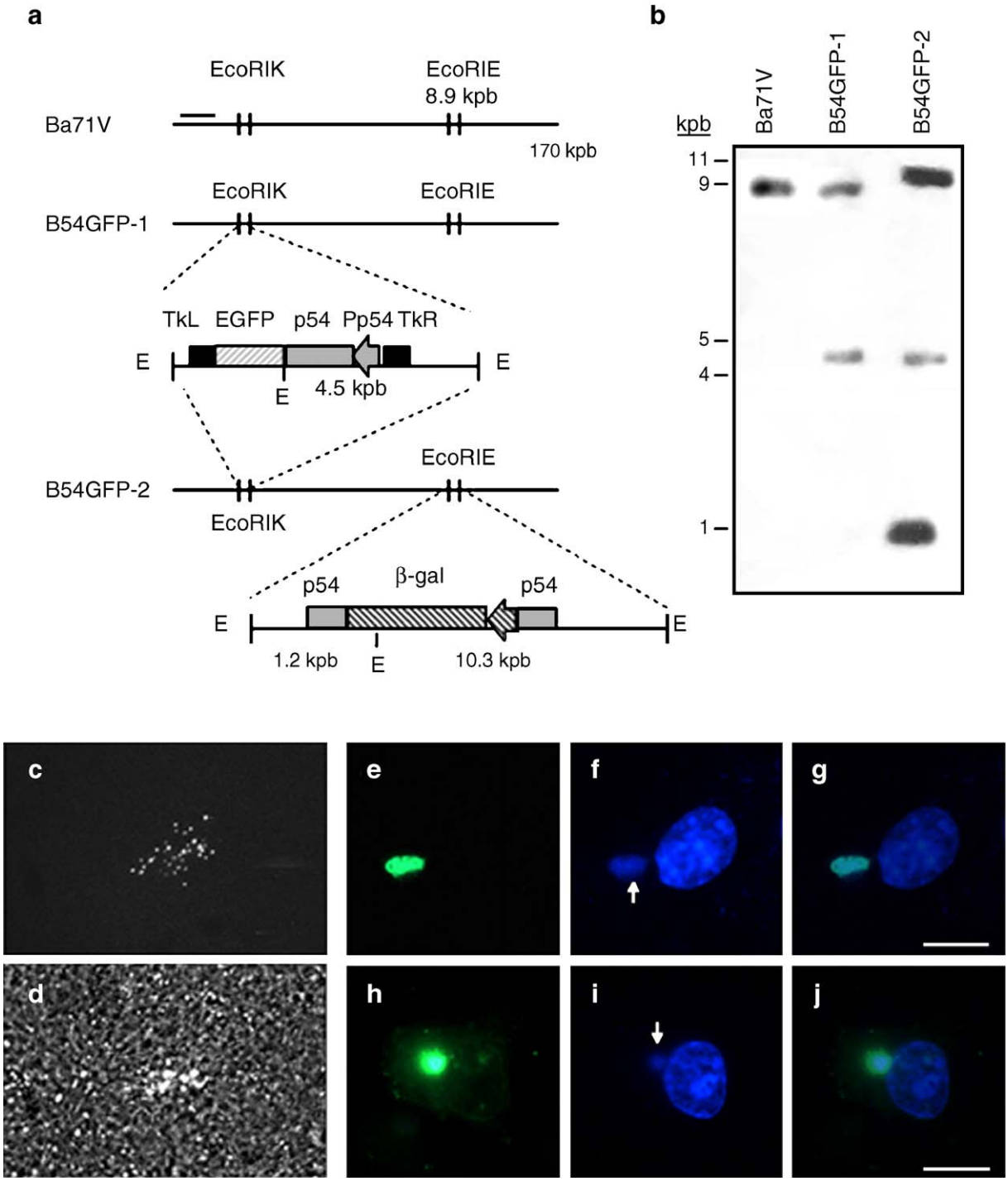

Fig. 1. Generation of fluorescent tagged ASFV. (a) Schematic representation of the *Eco*RIK and *Eco*RIE fragments in the genome of the wild type ASFV (BA71V) and the recombinants viruses generated (B54GFP-1 and B54GFP-2) after insertion of chimera p54-EGFP in *Tk* locus by homologous recombination and disruption of the p54 gene by insertion of the β-gal marker gene, as described in Methods. E: *Eco*RI site. (b) Genomic analysis, after *Eco*RI digestion, of parental and recombinant ASF viruses by Southern blot using a digoxigenin-11-dUTP labeled DNA probe corresponding to the p54 complete coding sequence. Size of the fragments probed was as expected after genome manipulations. (c and d) After insertion of p54-EGFP recombinants viral plaques formed in Vero cells monolayers exhibited fluorescence and allowed and easy detection after 5 dpi. (c) A single recombinant fluorescent plaque was photographed in a fluorescence microscope (original magnification ×100) and correspondent transmitted light image is shown below (d). Fluorescence microscopy analysis of B54GFP-1 (e–g) or BA71V infected cells at 14 hpi (h–j). p54-EGFP was performed by direct fluorescence (e), while p54 was detected with an anti-p54 serum and secondary antibody conjugated to Alexa 488 (h). In both cases viral and cellular DNA were counterstained with Hoechst to visualize viral factories, indicated by arrows (f and i). As it can be observed, in the merged images (g and j), p54-EGFP and p54 showed similar perinuclear distribution coincident with viral factories. Scale bar, 18 μm.

p54-EGFP is incorporated into intact infectious ASF virions

To determine that protein p54, a major component of the external envelope of ASFV, fused to EGFP protein remains incorporated to the viral particle, BA71V and B54GFP-2 virions were Percoll purified and analyzed by SDS-PAGE and Western blotting using specific antibodies (Fig. 2a). No reactivity of anti-GFP antibody with BA71V purified virus was found, while a 51-kDa band corresponding to the expected size of p54-EGFP protein was detected in B54GFP-2 purified virus. However, when an anti-p54 serum was probed, a 25-kDa band appeared with BA71V virus and with anti-GFP serum, a 51-kDa band was only reactive with the recombinant virus, demonstrating the incorporation of p54-EGFP fusion protein into the virus particles. The typical doublet detected with anti-p54 serum in BA71V samples was not present in those from B54GFP-2 when detection of p54-EGFP was carried out with monoclonal antibody anti-GFP. It is noteworthy that the levels of p54-EGFP and p54 incorporated into their respective particles were apparently equivalent, since the amount of total virus protein loaded in SDS-PAGE was similar in both cases, as judged by Coomasie blue staining. In order to further confirm this, we analyzed by Western blotting the presence of major structural ASFV protein p72 in these highly purified virions (Fig. 2a). The proportion of p54-EGFP relative to p72 in B54GFP-2 virions was roughly the same as p54/p72 rate inBA71V virions, indicating that the fusion protein was incorporated to virus particle at similar rates than p54.

Biological properties of B54GFP-2

To ascertain the growth properties of the B54GFP-2 virus, a time course of infection was carried out for both, wild-type and recombinant viruses. Monolayers of Vero cells were infected with BA71V or B54GFP-2 at a multiplicity of infection (moi) of 5 pfu/cell and harvested at different postinfection times. Total cell lysates were analyzed by SDS-PAGE and Western blotting, and the kinetics of synthesis of virus proteins were assessed (Fig. 3a). Western blotting with an anti-p54 serum allowed the identification of a 51-kDa band, the expected size for p54-EGFP, only in B54GFP-2 infected cell extracts from 8 to 24 hpi. At the same times postinfection,

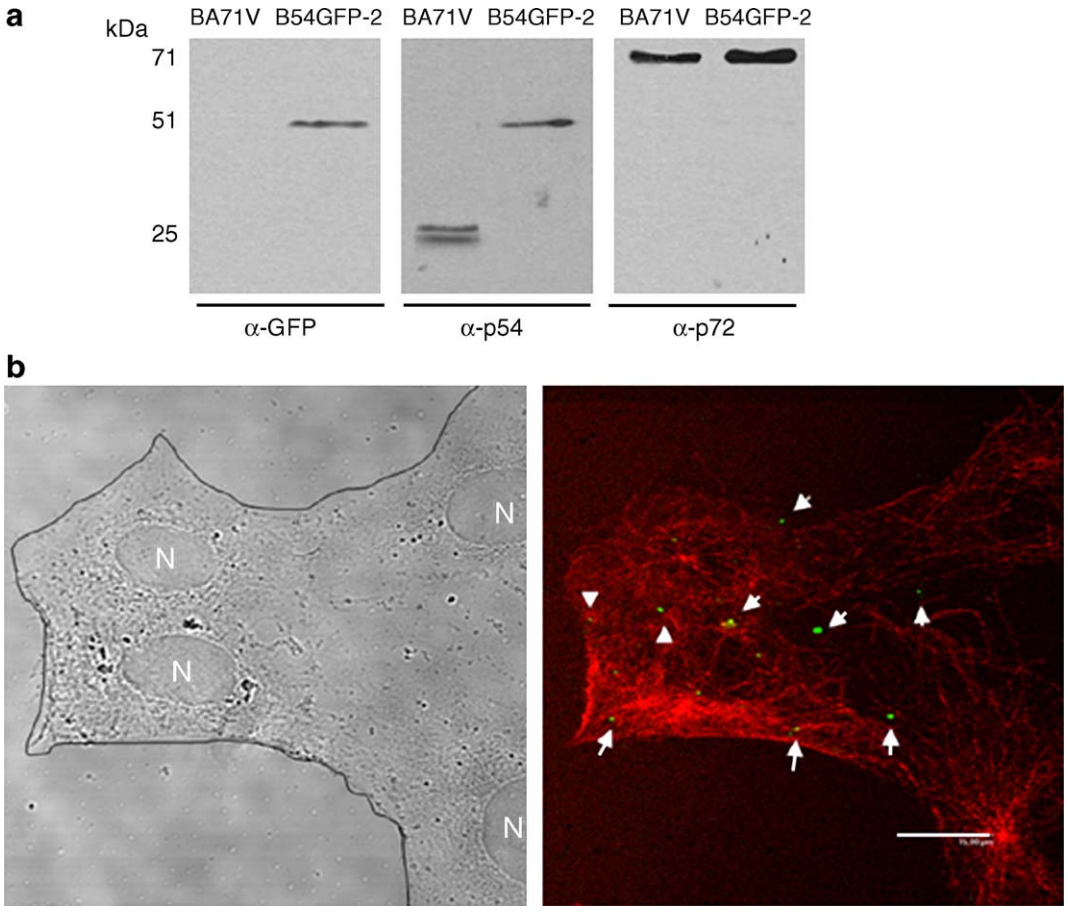

Fig. 2. Incorporation of p54-EGFP into B54GFP-2 virions. (a) BA71V and recombinant virus B54GFP-2 were purified from culture supernatants by Percoll equilibrium gradient sedimentation (see Methods). Fractions from gradient containing highly purified virus free of vesicles were pooled and lysed. Total protein contained in samples was estimated by Coomasie blue staining and equal amounts of protein from BA71V and B54GFP-2 samples were electrophoresed and analyzed by Western blot with specific antibodies: anti-GFP, anti-p54 and anti-p72. Proteins were separated by SDS-12% PAGE and revealed with chemiluminescence. (b) Right: B54GP-2 particles were detected by fluorescence confocal microscopy (indicated by arrowheads) at 30 min postinfection, in fixed Vero cells. β-tubulin was detected with monoclonal specific antibody (Alexa fluor 647). Left: correspondent phase image. N: cell nucleus. Continuous line shows cell outline. Scale bar, 18 μm.

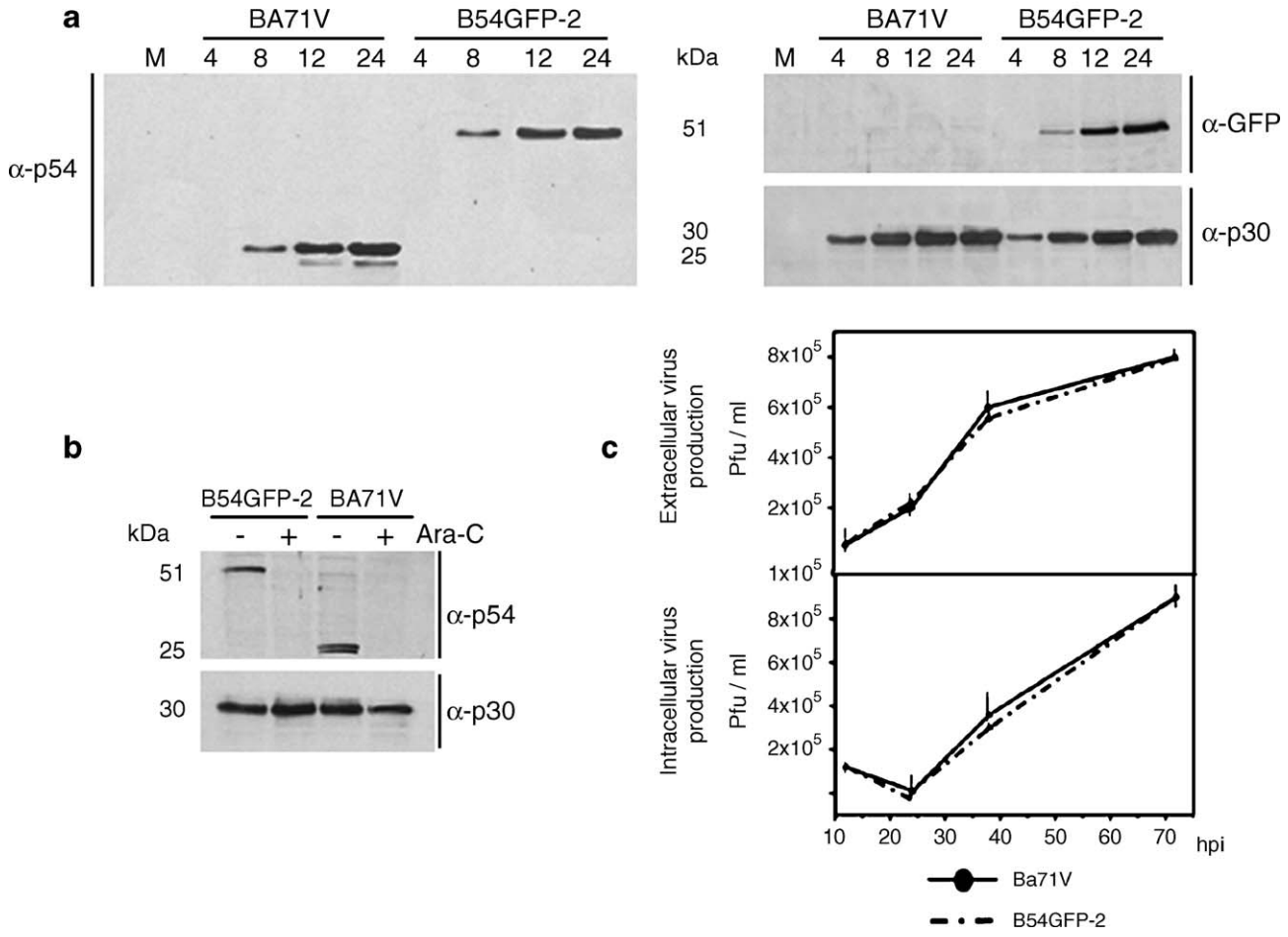

Fig. 3. Fusion to EGFP did not alter the intrinsic properties of protein p54. (a) Vero cell monolayers were infected with BA71V or B54GFP-2 at 5 pfu/cell. At indicated times cells were harvested and processed for analysis of diverse virus protein synthesis by Western blot with anti-p54, anti-GFP and anti-p30 (see Methods for dilutions). M: mock infected. (b) Cell monolayers were infected with BA71V or B54GFP-2 at 5 pfu/, in presence (+) or absence (−) of inhibitor cytosine β-arabinofuranoside (Ara-C) to discriminate late from early viral protein synthesis. Cells were harvested at 14 hpi and analyzed by Western blot with a serum anti-p54 that recognized p54-EGFP and p54 only in absence of Ara-C. Early ASFV protein p30 was detected in presence and absence of inhibitor using monoclonal antibody anti-p30. (c) Analysis of the replicative phenotype of B54GFP-2. Cells were infected with 0.1 pfu/cell of BA71V or B54GFP. Every 12 hpi (for a maximum of 72) extracellular and intracellular infectious virus progeny was estimated by plaque assays. Growth curve obtained for recombinant virus resulted similar to the parental virus BA71V.

p54 was detected as a doublet in BA71V infected cell extracts while a single 51 kDa band was detected with a monoclonal antibody against GFP, only in recombinant virus infected cell extracts at these time points. p54-EGFP apparently remained intact throughout the course of the infection and sample preparation, since no doublet was observed in WB. As expected, fusion protein was synthesized late after infection (detectable from 8 hpi by WB), in contrast to the early protein p30 used as a control, which was detected from 4 hpi. To demonstrate that p54-EGFP is synthesized during the late viral expression phase under the control of p54 promoter, we examined the synthesis of fusion protein in the presence and absence of a DNA replication inhibitor, such as cytosine β-arabinofuranoside (Ara-C). In the presence of Ara-C, we could detect neither p54-EGFP nor p54 with anti-p54 serum, while early ASFV protein p30 expression was confirmed by WB with a monoclonal antibody against p30 in the presence and absence of inhibitor (Fig. 3b).

These results demonstrated that virus gene expression was similar in B54GFP-2 and wild-type virus infected cells, but it was conceivable, since p54-EGFP is a structural component of the virus particle, that assembly and/or release from the cell of the double recombinant virus could be in some way restricted. To assess the rate of virus assembly and egress throughout several infection cell cycles, growth curves were carried out for both B54GFP-2 and the BA71V virus. Vero cells were infected at a multiplicity of 0.1 pfu/cell and harvested every 10 h for 72 h, and both extracellular and intracellular virus yields were calculated for both viruses. The results showed that the growth curves for extracellular and intracellular virus were similar for wild-type and recombinant virus infections, not only in total infectious virus production after 72 hpi, but at every time point we examined (Fig. 3c). These results imply that the rates of both virus assembly and virus egress from the cell were the same for the two viruses.

Individual B54GFP-2 virus particles detection

The incorporation of p54-EGFP into virions of the ASFV B54GFP-2 makes possible that these particles can be detectable by fluorescence. To test if this was the case, virions purified by sedimentation through sucrose cushion were used to infect Vero cells grown onto a coverslip at a multiplicity of 10 pfu/cell. After synchronizing the infection at 4 °C for 2 h, cells were incubated for 30 min at 37 °C and subsequently examined by fluorescence microscopy. Fluorescent particles, visualized as point sources of GFP fluorescence, were readily detected inside cell cytoplasm (Fig. 2b). When target cells were washed of free virus and allowed to incubate further at 37 °C, a significant proportion of the GFP signal accumulated in the perinuclear region, in a short time after infection 4 h (Additional file 1). Images were acquired at 30 min and 4 h postinfection, before late viral protein expression phase onset to avoid that observed GFP signal corresponds to newly synthesized p54-EGFP.

p54-EGFP distribution in the viral factory in late infected cells

Some obvious applications of a virus expressing a fluorescent structural protein would be to localize that protein within the cell and follow its trafficking during the infection cycle and ultimately, to visualize the pathway of virus assembly in live cells. As previously shown, wild-type p54 and p54-EGFP distribution at late times in wild type and B54GFP-1 infection was shown in perinuclear viral factories (Figs. 1e–j). We examined this distribution for B54GFP-2 infected cells at 12–16 hpi by confocal fluorescence microscopy in fixed cells (Figs. 4a–d). Protein p54-EGFP distribution coincided with assembly sites in the viral factories, which is characterized by a great accumulation of newly synthesized viral DNA. To further confirm that p54-EGFP distribution could be used as a novel viral factory marker in ASFV infection we showed that the Golgi complex in living B54GFP-2 infected cells was located surrounding, but not coincident with the viral factory where a great accumulation of p54-EGFP is found (Figs. 4e–g).

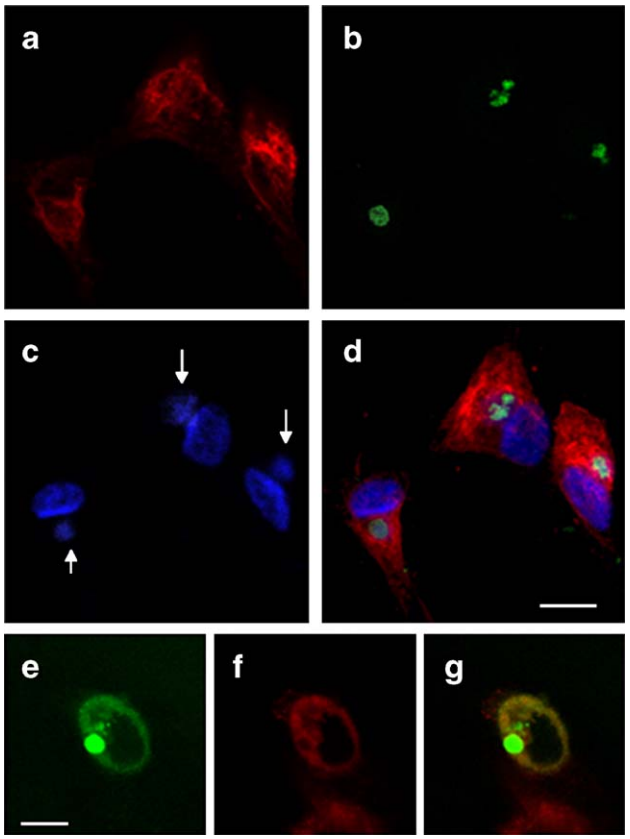

Fig. 4. p54-EGFP intracellular distribution at the viral factory in B54GFP-2 infection. Vero cells infected with B54GFP-2 were analyzed by confocal immunofluorescence microscopy at 12 hpi (a–d). (a) β-tubulin was labeled with monoclonal anti-β-tubulin antibody conjugated to Alexa 647, while p54-EGFP was detected by direct fluorescence (b). Staining of viral and cellular DNA with Hoechst 33342 (c) allowed the identification of perinuclear viral factories (indicated by arrows) where replication of ASFV DNA occurs. (d) Colocalization of p54-EGFP with viral factories is shown in the merged imaged. (e–g) Golgi complex was detected in B54GFP-2 infected live cell, by staining with Bodipy-TRC$_5$-ceramide (f). Merged imaged (g) shows the perinuclear distribution of Golgi complex surrounding p54EGFP (e), but not coincident. Scale bar, 20 μm.

Time lapse analysis of virus infection

The ultimate elegance of a GFP-incorporating virus is the potential for monitoring virus infection in individual living cells. The abundant incorporation of p54-EGFP into ASFV particles indicated that it should be possible to visualize the intracellular movement of virions in real time by laser-scanning confocal microscopy of live cells. Approximately 50% confluent Vero cells were infected with more than 10 PFU of B54GFP-2 virus per cell. Virus infection was synchronized by incubation of cells at 4 °C for 90 min and images were collected, after incubation at 37 °C for nearly 2 h, to analyze the first steps of infection at high magnification. Individual virus particles were readily observed and images were acquired with the confocal microscope setup at a rate of 1 frame/3s for a maximum of 2 min. With this short interval of time, we discerned that intracellular movement in the proximity of perinuclear areas was composed of frequent stops and starts, and often without any apparent direction. Fig. 5 shows an example of this intermittent or saltatory movement of an individual virion. Over the times and distances measured in following frames acquired from 10 different virions, an average speed ranged from 0.2 to 0.5 μm/s at this stage of infection was calculated. In order to test the role of microtubules at this stage of infection, disruption of microtubules with 10 μM nocodazole was achieved prior to infection with B54GFP-2. Under these conditions we could not track any virion movement examined at 1 hpi or 4 hpi in live cells. Interestingly, at mentioned times postinfection most GFP signal was localized far from perinuclear areas in contrast to infected cells with intact microtubules (Additional file 2).

To determine the stage of infection at which newly synthesized p54-EGFP could initially be detected by direct fluorescence microscopy, and to visualize virus factory constitution, Vero cells were infected with B54GFP-2 at a multiplicity of infection of 1 pfu/cell. After synchronization of the infection, cells were examined for EGFP fluorescence every

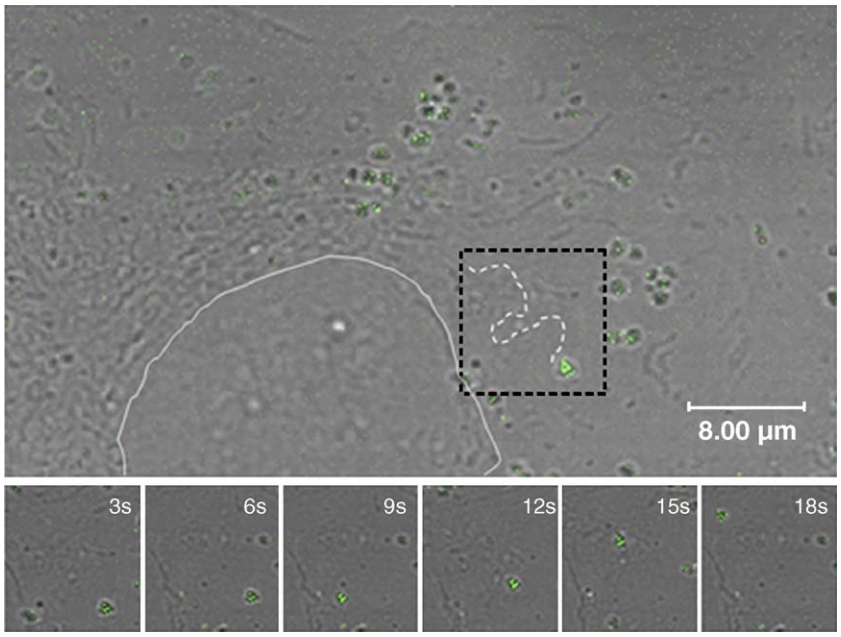

Fig. 5. Analysis of the intracellular movement of B54GFP-2 viral particles. Vero cells were B54GFP-2 infected with 20 pfu/cell and examined by confocal microscopy at 1 hpi, acquiring images every 3 s corresponding to 0.5 µm optical sections from the Z axis. Virus particles were detected as EGFP point sources, and correspondent transmitted light image provided points of reference information. Movement of 10 virions were individually analyzed. Upper image shows an example of the trajectory followed by one of the virions analyzed (white discontinuous line) and selected area is enlarged below. Total distance covered by this virion was 11.74 µm in 30 s, with an average speed of 0.5 µm/s. As can be observed in the figure, virion velocity was not constant, with a maximum speed from 12 to 15 s. Scale bar, 8µm as indicated.

5 min over a period of 18 h by live cell confocal microscopy. Representative images collected at indicated time points are shown in Fig. 6. Protein p54-EGFP was first observed in the majority of cells as early as 7–8 hpi. The protein was mainly localized as small, cytoplasmic and fluorescent aggregates around the nucleus (2 or 3 spots were usually observed within single cell). From this point, all of these perinuclear spots finally aggregated along the next 2 h to give rise to a unique brilliant spot close to the nucleus (Fig. 6b). This accumulation of p54-EGFP, which was previously shown coincident to the viral factory, gradually increased in size and fluorescence intensity as infection proceeded. It should be mentioned that aggregation of initial perinuclear spots of p54-EGFP could not be observed in every infected cell, but in most of them, probably due to changes in the optical section acquired during the monitoring of the infection. At late times postinfection, in most of the cells, it was usually to observe violent changes in viral factories location (Fig. 6a), however these changes seem to correspond to movements of infected cell prior to detachment from the dish, while factory location is conserved.

In another set of experiments, we investigated the relationship, of mitochondria status and viral factory formation in a time course manner. At initial infection steps mitochondria were observed as an almost continuous succession of organelles extending throughout the cytoplasm. Nevertheless, time lapse experiments with image acquisitions every 5 min in Vero cells infected at a moi of 1 pfu/cell, showed the progressive alteration of the normal mitochondrial pattern and mitochondrial irregular clumping and aggregation around viral factory was observed (Fig. 8). This aggregation started at 8 h after infection, coincident with p54-EGFP synthesis, suggesting the high energy requirements of the virus assembly process.

Apoptosis has been described to play an important role in ASFV pathogenesis (Ramiro-Ibanez et al., 1996), so we decided to analyze the very late stages of ASFV infection in living cells infected with B54GFP-2. Fig. 7 shows in detail the characteristic morphological changes that occur during programmed cell death of an infected cell. Since 12 hpi an early cytopathic effect, consisting in cytoplasmic vacuolization, rounding and reduction in the size of the infected cell was be observed. From this time point onwards, the cell lost contacts with neighboring cells and detached from the monolayer, undergoing nuclear fragmentation and final cell death. This process included typical membrane blebbing of the infected cell that led to the formation of numerous vesicles containing large amounts of p54-EGFP. Vesicle formation has been considered a very characteristic feature of ASFV infection in cultured cells and these are virus-containing vesicles. Completion of the process from the first morphological features of apoptosis lasted around 6 h.

Discussion

Successful African swine fever virus life cycle is dependent on several and critical interactions with host cell which remain poorly understood. Some of these events include virus internalization into cellular cytoplasm, transport to perinuclear areas where viral DNA replication occurs, egress of viral progeny from assembly sites to cell periphery and virus induced cell death. Recent improvements in optical imaging techniques combined with protein fusion to GFP variants, open new

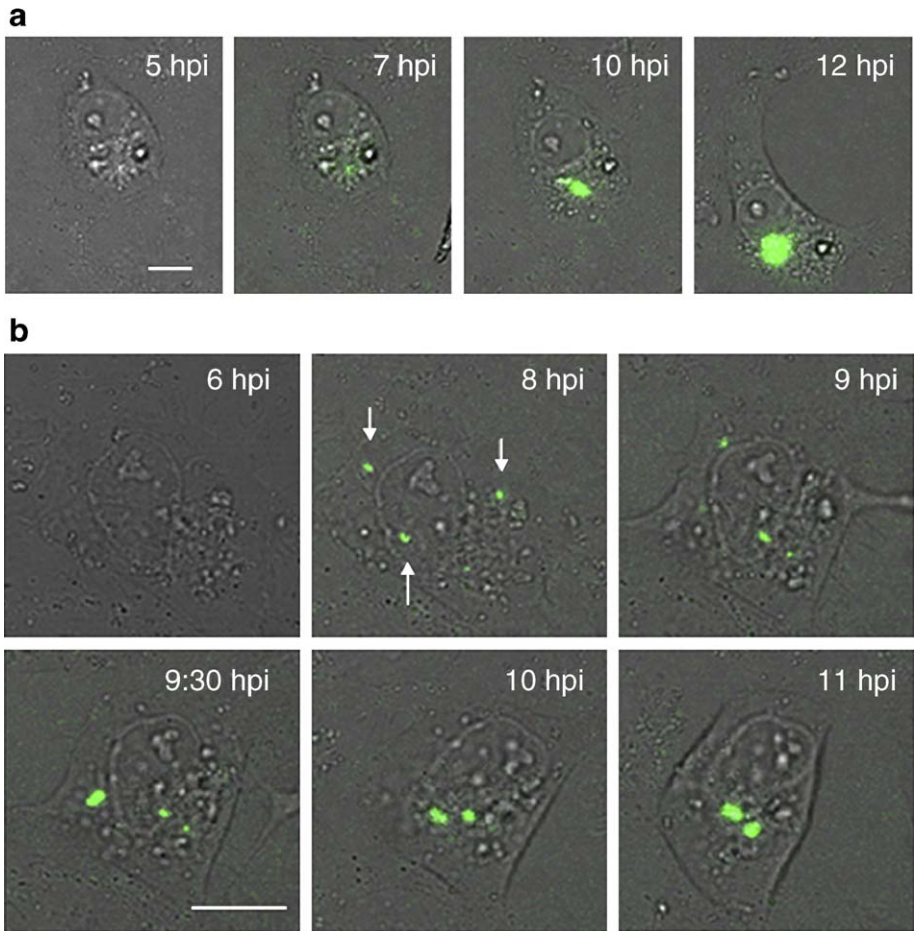

Fig. 6. Constitution of the viral factory in B54GFP-2 infected live cells. Vero cells were B54GFP-2 infected with 1 pfu/cell. After infection synchronization, cells were maintained at 37 °C for the complete image acquisition period. (a) p54-EGFP (green) and transmitted light images of the same B54GFP-2 infected cell were simultaneously acquired by confocal microscopy at indicated times postinfection. The progressive accumulation of p54-EGFP in perinuclear areas from 7 hpi and the violent movements of the infected cell prior to detachment from dish are observed. Scale bar, 18 μm. (b) Images, collected in the same way, from 6 hpi show the aggregation of several perinuclear and bright p54-EGFP spots (indicated by arrowheads in 8 hpi image) that resemble aggresomes, to constitute a unique and final viral factory in the infected cell. Scale bar, 20 μm. (For interpretation of the references to colour in this figure legend, the reader is referred to the web version of this article.)

possibilities for the direct analysis of these dynamic processes. This new methodology has been successfully applied to study different aspects of the infection of adenoviruses (Lux et al., 2005), herpesviruses (Glotzer et al., 2001; Sampaio et al., 2005), poxviruses (Geada et al., 2001; Hollinshead et al., 2001; Ward and Moss, 2001), rhabdoviruses (Finke et al., 2004) or retroviruses (McDonald et al., 2002; Muller et al., 2004). We reported here the generation of a fluorescently tagged and viable ASFV expressing the structural protein p54 as an EGFP fusion protein. Expression of p54-EGFP enables easy identification of infected cells by direct fluorescence analysis, which results useful when immunodetection of diverse antigens in the same sample is desirable.

Selection of p54 as the viral fusion protein was supported by several reasons. Since p54 is located in the inner viral envelope (Rodriguez et al., 1994), fluorescent p54 would allow the detection of individual viral particles upon infection. As the carboxi- terminal tail of p54 is facing the surface of mature virions, it was expected to be a suitable target for EGFP fusion. On the other hand, newly synthesized p54 accumulates within perinuclear areas where morphogenesis takes place at late times postinfection. Thus, p54-EGFP could become a very helpful tool to analyze viral factories assembly.

The strategy to generate tagged virus B54GFP-2, consisted in two sequential steps. After initial insertion of p54-EGFP coding sequence under the control of p54 promoter, it was found that fusion of EGFP to the C-terminus of p54 did not affect the perinuclear subcellular distribution of the viral protein, as it was directly observed in B54GFP-1 infected cells. Then, we interrupted *E183L* gene in B54GFP-1 genome by insertion of β-galactosidase coding sequence as second selection marker, to ensure that every p54 molecule that accommodates in virion inner envelope would be EGFP tagged. Previously, p54 has been shown to be essential for virus viability, playing and important role in ASFV morphogenesis (Rodriguez et al., 1996, 2004), so the recovery of recombinant virus B54GFP-2 after wild type p54 interruption indicated that fusion did not apparently affect the normal function of p54. Furthermore, growth curves obtained with recombinant virus indicated identical replication behavior and infectious efficiency when compared to the parental strain.

Furthermore, fusion to EGFP did not alter the expression pattern determined by WB analysis for p54 in infection as p54-

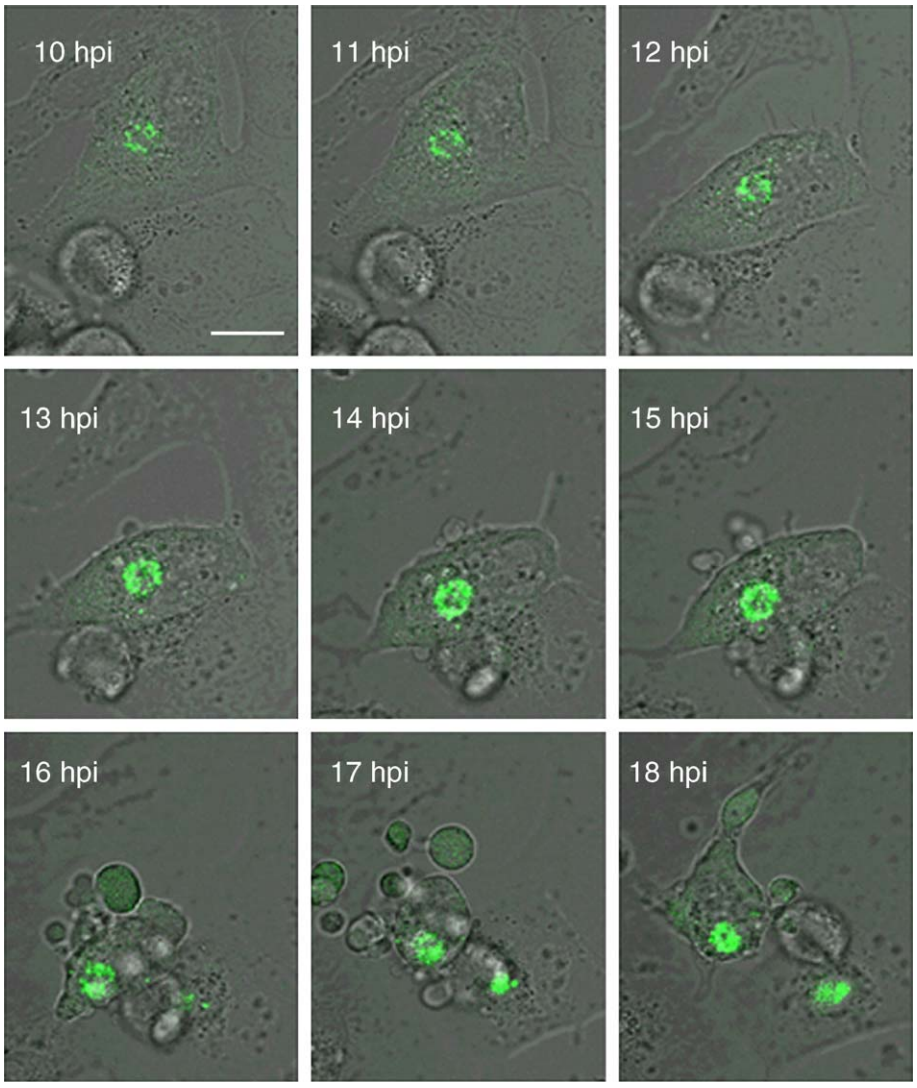

Fig. 7. Live-cell analysis of the last stages of B54GFP-2 infection. Series of EGFP and transmitted light simultaneous acquisitions of the same B54GFP-2 infected Vero cell by confocal microscopy from 10 hpi (when viral factory is already constituted) and every 5 min (see additional file 3 to complete animation sequence). Rounding of the infected cell is followed by membrane blebbing and subsequent formation of p54-EGFP (green) containing vesicles. At 18 hpi, detachment and final cell destruction is observed. Scale bar, 20 μm. (For interpretation of the references to colour in this figure legend, the reader is referred to the web version of this article.)

EGFP expression remained under control of p54 natural promoter in B54GFP-2. P54-EGFP was synthesized and detected during late viral expression phase, from 8 hpi, as expected. This observation was confirmed by WB analysis in the presence of inhibitor Ara-C, which demonstrated that there was not chimera protein expression when viral DNA replication was inhibited. Also, expression levels of p54-EGFP in infection, determined by WB, did not apparently differ from those observed for p54.

In order to track single fluorescent ASFV particles, it is an essential requirement that p54-EGFP is incorporated into viral particles. Previously, p54 has been successfully used as a target to generate ASFV chimeras incorporating short foreign viral epitopes such as the antigenic site A from foot-and-mouth disease virus VP1 protein and the DA3 antigenic determinant from transmissible gastroenteritis coronavirus nucleoprotein N (Brun et al., 1999). In both cases, chimeric p54 proteins were successfully incorporated into the viral particles, supporting selection of p54 as the fusion protein. As expected, Western blot with Percoll purified B54GFP-2 particles demonstrated the association of p54-EGFP with ASFV virions. As deduced from detection of control protein p72 and p54 in Percoll purified samples, inclusion of p54-EGFP into virions appeared to occur with same effectiveness than p54.

Such tagged virus will enable live analysis of various stages in the ASFV replicative cycle using confocal microscopy. One of these potential applications of B54GFP-2, shown in present work, would be the analysis of intracellular movements of fluorescent particles during the initial phase of infection immediately after internalization into the host cell. When collecting confocal microscopic images every 3 s, from 2 hpi, it was found that most of the viral particles exhibited a special kind of movement defined as saltatory, intermittent and apparently disorganized, making difficult the estimation of

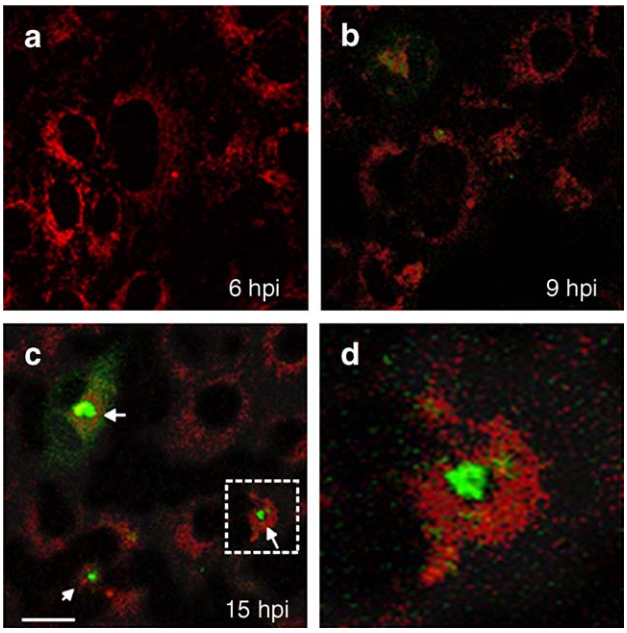

Fig. 8. Live-cell analysis of mitochondria in B54GFP-2 infection. Vero cells were infected with 1 pfu/cell and synchronization of infection was achieved. Live mitochondria (red) were detected with CMXRos. (a) At early stages of infection, mitochondria are disposed as a continuous ring throughout the cytoplasm. (b) Initial aggregation of mitochondria around newly synthesized p54-EGFP (green) was observed since 8 hpi. (c) Aggregation of mitochondria around virus factories can be observed in late infected cells (indicated by arrows), while disposition of mitochondria in non infected cells is typical of healthy cells. Selected area is enlarged in image d. Images were acquired by confocal fluorescence microscopy every 5 min from 6 hpi. Scale bar, 20 μm. (For interpretation of the references to colour in this figure legend, the reader is referred to the web version of this article.)

speed rates. This type of movement has been described as characteristic of microtubule associated movement. From the analysis of movement of 10 individual virions an average speed ranging from 0.2 to 0.5 μm/s was calculated with the applied resolution. These data are in agreement with those obtained for other large enveloped viruses. Using fluorescence videomicroscopy, which allows a resolution of 1 frame/s, speed rates from 0.3 to 1 μm/s have been determined during the late phase of infection with labeled vaccinia virus (Geada et al., 2001; Ward, 2005; Ward and Moss, 2001). Recently, human cytomegalovirus has been shown to move with apparent velocity of 0.7 to 0.8 μm/s (Sampaio et al., 2005) at very early stages in infection. Moreover, HIV virions transport towards host cell nucleus linked to microtubules occurs at 1 μm/s (McDonald et al., 2002). The saltatory movements of tagged ASFV virions and the speed rates obtained are consistent with a microtubular based transport (King, 2000) and association of this virus with microtubules has been described (de Matos and Carvalho, 1993). Previously, we identified the LC8 subunit of cytoplasmic dynein, a minus end directed microtubule-associated motor protein, as an interacting protein with p54 (Alonso et al., 2001), resulting this interaction critical in the first stages of ASFV infection. Collectively, these data suggested a role for microtubules in the intracellular transport of ASFV after internalization. This role is supported by data showing that nocodazole disruption of microtubules prior to infection results in stop of virion movement and lack of perinuclear accumulation of viral particles at 4 hpi that remained dispersed in the cytoplasm. Also, there was no subsequent constitution of the characteristic virus factory and finally a reduction in ASFV progeny was found (additional files 1 and 2 and Alonso et al., 2001). Also, during the late phase of ASFV infection, transport of newly assembled virions from viral factory to cell periphery along microtubules has been recently demonstrated (Stefanovic et al., 2005), similar to the exit transport described for vaccinia virus (Carter et al., 2003). Further live studies involving labeled B54GFP-2 that are now in course will provide useful and detailed information to clarify the whole ASFV penetration and egress process into the host cell.

P54 has been previously described to localize in membrane structures within the virus factories and in immature ASF virions, as judged by immunogold electron microscopy (Rodriguez et al., 1994). P54-EGFP, just as p54, showed an intracellular distribution fully coincident with ASFV factory at late postinfection times. This allowed us, to follow the viral factory formation process in live cells throughout the infection cycle for first time. Animations obtained show that p54-EGFP was first detected in cytoplasm as several discrete and bright spots representing initial viral assembly sites. As infection progresses these initial assembly sites migrated to a perinuclear area, fused and finally formed a single large accumulation of p54-EGFP per cell. Similar assembly sites were previously described as viral antigens inclusions containing viral precursors which remained tightly associated to microtubules (Carvalho et al., 1988). Indeed, microtubule associated motors are required to transport these initial assembly sites towards the microtubule organization center (MTOC), where final ASFV factory is constituted (Alonso et al., 2001; Heath et al., 2001) following viral replication and viral assembly takes place. First steps in ASFV assembly consist in the modification of ER membranes (Andres et al., 1998; Rouiller et al., 1998). Protein p54 has been involved in the recruitment to the viral factories and transformation of the ER-derived envelope precursors that are finally acquired by virions (Rodriguez et al., 2004). This new role for p54 in morphogenesis supports the selection of p54 as viral fusion protein and suggests that studies about p54-EGFP trafficking during infection in live cells would be helpful to analyze the acquisition of ASFV envelopes from ER during virus assembly.

The formation of the viral factory often involves not only host cytoplasmic membranes and cytoskeletal components, but also cell organelles such as mitochondria. These are thought to play an important role in several large DNA enveloped virus infections (Murata et al., 2000; Novoa et al., 2005; Rojo et al., 1998), supplying the energy required in the morphogenetic and assembly processes. Our results, obtained with live ASFV infected cells have confirmed these previous observations in fixed cells (Hernaez et al., 2004a; Rojo et al., 1998), which showed that ASFV infection induce the migration of mitochondria to the perinuclear assembly sites, producing the clustering of this actively respiring organelle around viral factory. This migration occurs since 8 hpi, before the definitive viral factory is fully constituted, suggesting that energy

contribution from mitochondria is required since first stages of ASFV morphogenesis.

Finally, we analyzed the destruction of the ASFV infected cell. This process started at 12 hpi and usually lasted about 6 h, being identical to apoptotic cell death, which has been demonstrated to play a relevant role in ASFV pathogenesis (Hernaez et al., 2004a, 2004b; Ramiro-Ibanez et al., 1996). In live cells, it was possible to observe host cell membrane blebbing, resulting in the formation of p54-EGFP containing vesicles. This finding raised the possibility that these vesicles could contain virus particles. Previous publications reported that the abundant vesicle fraction released in last ASFV infection stages contains virus (Carrascosa et al., 1985). Then, it is conceivable that the fluorescence detected in the vesicles formed at the end of apoptosis (blebbing), could correspond to GFP labeled virus particles. This vesicle formation observed in live cells is rarely observed using common fixation methods, then it is not possible to observe it with the parental unlabeled virus.

In summary, we have generated a fluorescently tagged ASFV, which could be a powerful tool since it enables live analyses of diverse aspects of ASFV live cycle, including viral particles intracellular transport, morphogenesis and apoptosis of the infected cell. We presented here, for the first time, live images of some of these stages in ASFV infection and more detailed information will arise from future and novel studies of virus entry and egress.

Methods

Cells, viruses and plasmids

Vero cells were obtained from ECACC and grown at 37 °C in a 5% CO_2 atmosphere in Dulbecco's modified Eagle's medium (DMEM) supplemented with 5% foetal bovine serum (FBS). ASFV isolate BA71V, adapted to grow in Vero cells, was used in infection experiments carried out at 37 °C and 5% CO_2. When synchronization of infection was required, this was performed for 90 min at 4 °C after viral inoculum was added. In most cases, ASFV stocks from culture supernatants were semipurified from vesicles by ultracentrifugation at 40.000 × g through a 20% (w/v) sucrose cushion in PBS for 1 h at 4 °C. When needed, ASFV particles were highly purified from the extracellular medium by Percoll equilibrium centrifugation as previously described (Carrascosa et al., 1985). After centrifugation, Percoll gradients were fractionated and fractions 2 to 8 from Percoll gradients, containing virus particle essentially free of vesicles and contaminant membranes, were collected after sedimentation and gel filtered through Sephacryl S-1000 (Amersham) to remove Percoll.

The construction of the insertion vector pINS-54EGFP involved several steps. The expression plasmid pEGFP-N1 (Clontech) was used as template to obtain the EGFP coding sequence by PCR with specific primers (5′-CGCGGATCCGC-AGTAAAAAAATG-3′ and 5′-CGCGGAATTCATGGTGAG-CAAGGGC-3′). A fragment of 800 pb corresponding to p54 promoter and complete p54 coding sequence was also obtained from BA71V genome by PCR with specific primers (5′-GCGGGATCCCGTTGTCTAGGTAA-3′and 5′-GCGGAATT-CCAAGGAGTTTTCT AGG-3′). In order to generate the vector pINS-54GFP, previous PCR products were digested with *Eco*RI and *Bam*HI and cloned into the 4.7 kpb fragment resulting from the digestion of plasmid pINS72Gal (Gomez-Puertas et al., 1995; Rodriguez et al., 1992) with *Bam*HI.

The construction of the vector pΔp54, used to perform the interruption of E183L gene, was described previously (Rodriguez et al., 1996). Briefly, this vector contains β-galactosidase coding sequence under control of p72 promoter, flanked by two fragments from *E183L* that allow homologous recombination with this ORF in BA71V genome. These flanking sequences correspond to 424 pb and 888 pb from right and left extremes from p54 gene, respectively.

Construction of B54GFP-2

An African swine fever virus recombinant expressing an enhanced version of the GFP gene (EGFP) fused to the C-terminus of the p54 coding sequence was constructed in two steps: first, the insertion of the p54-EGFP coding sequence into thymidine kinase locus (TK) in BA71V genome was achieved by homologous recombination after transfection of Vero cells with pINS-p54EGFP in the presence of Fugene (Roche), according to manufacturer's instructions. Eight to 16 h after transfection, cells were infected with BA71V at a moi of 0.1 pfu/cell. When the cytophatic effect was complete (approximately 72 hpi) the cultures were harvested and sonicated. These transfection-infection mixtures were used to infected monolayers of Vero cells seeded onto 100 mm dishes (Nunc) at different dilutions. After 5–6 dpi, the recombinant virus generated was isolated from progeny virus by three rounds of plaque purification on Vero cells, during which recombinant virus plaques were screened for EGFP direct fluorescence. The resulting recombinant virus was named B54GFP-1. Additional second step consisted in the inactivation of the original gene of p54 (*E183L*) in the B54GFP-1 genome to finally generate the recombinant virus B54GFP-2. The transfection of Vero cells with pΔp54 and following infection with B54GFP-1 allowed the insertion of the β-galactosidase coding sequence downstream of the strong p73 promoter within E183L gene. Isolation of B54GFP-2 was performed as described above, screening recombinant virus plaques for EGFP fluorescence and expression of β-galactosidase (Gomez-Puertas et al., 1995).

The genomic structure of these recombinant viruses was confirmed by DNA hybridization analysis and could be observed in Figs. 1a and b. Briefly, DNA from parental and recombinant viruses were obtained and purified as previously described (Esposito et al., 1981). Resulting fragments, after *Eco* RI digestion, were resolved by agarose gel electrophoresis and then blotted onto uncharged Nylon membranes (Amersham). Membranes were probed with a digoxigenin-11-dUTP labeled DNA fragment corresponding to the complete p54 coding sequence. Final detection of digoxigenin was performed with CSPD (Roche) after probing the membrane with specific monoclonal antibody anti-digoxigenin (Roche).

Virus growth curves and plaque assays

Preconfluent monolayers of Vero cells were infected with either recombinant B54GFP-2 or parental BA71V at 0.1 pfu/cell. After 90 min, inoculum was removed and cells were washed with fresh DMEM and overlaid with DMEM supplemented with 2% FBS. Infected cells with their culture supernatants were harvested at different times postinfection (0, 12, 24, 48 and 72 hpi) and centrifuged at 3000 × g for 10 min. Cell pellets was resuspended in DMEM. Both the cellular fraction and the supernatant were sonicated and separately titrated by plaque assay to determine the intracellular and extracellular virus production respectively.

Plaques assays were performed as described previously (Gomez-Puertas et al., 1995). When isolation of recombinant virus plaques was desired, detection of EGFP fluorescence and expression of β-galactosidase were performed at 4 and 6 days postinfection respectively.

Immunoblot analysis

Vero cells preconfluent monolayers seeded on 6-well plates were infected with BA71V or B54GFP-2 at a moi of 5 pfu/cell. When inhibition of late viral protein synthesis was required, cells were incubated with cytosine β-arabinofuranoside (Ara-C) 50 μg/ml at 3 hpi. In all cases, cells were washed with PBS and harvested at 0, 4, 8, 12 and 24 hpi and lysed in RIPA buffer. After centrifugation at 10,000 × g for 20 min, proteins from cleared lysates were electrophoresed in 12% SDS-polyacrylamide gels and transferred to nitrocelluose membranes (BioRad). Membranes were incubated for 2 h at room temperature in PBS containing 5% non-fat dry milk and then probed with corresponding primary antibodies: monoclonal antibody anti p30 diluted 1:500, monoclonal antibody anti-GFP diluted 1:2500 (Clontech), and specific serum against p54 raised in rabbit diluted 1:1000, for 1 h at room temperature in PBS containing 0.05% Tween 20 (PBS-T). After extensive washing with PBS-T, membranes were incubated with anti mouse IgG antibody (diluted 1:5000) conjugated to horseradish peroxidase (Amersham) or anti rabbit IgG (diluted 1:4000) conjugated to horseradish peroxidase (Amersham).

In other experiments, proteins from ASFV highly purified particles were analyzed by Western blotting in the same way, but membranes were probed with monoclonal anti-GFP antibody, monoclonal anti-p72 antibody and polyclonal specific antibody anti-p54 raised in rabbit (diluted 1:1000). Anti mouse IgG antibody (diluted 1:5000) and anti rabbit IgG antibody (diluted 1:4000) conjugated to horseradish peroxidase (Amersham) were used as secondary antibodies respectively. In all cases, final detection on membranes was performed with ECL Western detection reagent (Amersham) and exposure to X-ray films (Kodak).

Fluorescence microscopy of fixed cells

Vero cells were grown on coverslips at 50–60% confluency and then infected with BA71V or recombinant viruses at different moi depending on the experiment. At desired time postinfection cells were rinsed twice with PBS and fixed with PBS containing 4% paraformaldehyde for 10 min at room temperature. When permeabilization was required, cells were incubated in presence of 0.1% Triton X-100 for 15 min at room temperature. A monospecific antiserum against p54 was raised in rabbit and used to visualize p54 (diluted 1:300). To detect tubulin a monoclonal antibody against β-tubulin (Sigma) was used (diluted 1:200). Secondary antibodies used were an anti rabbit IgG antibody conjugated to Alexa 488 fluor (Molecular Probes) and anti mouse IgG antibody conjugated to Alexa fluor 647 (Molecular Probes). Specificity of labeling and absence of signal crossover were determined by examination of single labeled control samples. p54-EGFP was directly observed by detection of fluorescence at λ = 509 nm. Nuclei as well as DNA in virus factories were detected by staining with Hoechst 33342. Finally, cells were mounted onto slides using Fluorsave reagent (Calbiochem).

Conventional microscopy was carried out in a Leica photomicroscope with a digital camera, and digitized images were obtained with Qwin software (Leica). Confocal microscopy was carried out in a Leica confocal microscope TCS SP2-AOBS equipped with a 63 or 100× objectives.

Fluorescence microscopy of live cells

Vero cells were plated at 60% confluence onto 35 mm dishes (WillCo Wells) and infected with 1 or 20 pfu of B54GFP-2 per cell, depending on the experiment. For the majority of experiments, synchronization of virus infection was achieved by performing the adsorption at 4 °C for 90 min and following removal of unbound virus. At indicated time points, cells were imaged by confocal microscopy carried out in a Leica confocal microscope TCS SP2-AOBS. In either case, cells were maintained on a heated 35 mm stage with the temperature set at 37 °C and fresh DMEM supplemented with 2.5% fetal bovine serum was perfused onto the dish at a rate of 0.1 ml/min throughout the experiment. The acquisition of images was every 5 min in long experiments (4 to 8 h length) and every 2–3 s in shorter experiments (from 1 to 4 hpi). Nevertheless, in long experiments only indicated postinfection times images are shown in figures. Simultaneous acquisition of EGFP fluorescence emission and transmitted light was performed. Microtubules depolymerization was achieved with 10 μM nocodazole (Sigma) 2 h before the infection without removing it during the acquisition of images. Detection of mitochondria in live cells was carried out with MitoTracker Red CMXRos (Molecular Probes) 100 nM for 30 min after virus infection. Golgi complex was detected in live cells with 5 μM Bodipy-TRC_5-ceramide complexed to BSA (Molecular Probes) for 30 min before infection, and emission detected at λ = 617. Manipulation and subsequent analysis of acquired images were carried out with Leica Confocal Software v.2.0.

Acknowledgments

This study was supported by grants from the Spanish Comisión Interministerial de Ciencia y Tecnología projects AGL2002-00668, AGL2004-07857-C03-03, BIO2004-00690 and BIO2005-0651.

Appendix A. Supplementary data

Supplementary data associated with this article can be found in the online version at doi:10.1016/j.virol.2006.01.021.

References

Alonso, C., Miskin, J., Hernaez, B., Fernandez-Zapatero, P., Soto, L., Canto, C., Rodriguez-Crespo, I., Dixon, L., Escribano, J.M., 2001. African swine fever virus protein p54 interacts with the microtubular motor complex through direct binding to light-chain dynein. J. Virol. 75, 9819–9827.

Andres, G., Simon-Mateo, C., Viñuela, E., 1997. Assembly of African swine fever virus: role of polyprotein pp220. J. Virol. 71, 2331–2341.

Andres, G., Garcia-Escudero, R., Simon-Mateo, C., Viñuela, E., 1998. African swine fever virus is enveloped by a two-membraned collapsed cisterna derived from the endoplasmic reticulum. J. Virol. 72, 8988–9001.

Andres, G., Alejo, A., Simon-Mateo, C., Salas, M.L., 2001. African swine fever virus protease, a new viral member of the SUMO-1-specific protease family. J. Biol. Chem. 276, 780–787.

Andres, G., Garcia-Escudero, R., Salas, M.L., Rodriguez, J.M., 2002. Repression of African swine fever virus polyprotein pp220-encoding gene leads to the assembly of icosahedral core-less particles. J. Virol. 76, 2654–2666.

Breese Jr., S.S., Pan, I.C., 1978. Electron microscopic observation of African swine fever virus development in Vero cells. J. Gen. Virol. 40, 499–502.

Brookes, S.M., Sun, H., Dixon, L.K., Parkhouse, R.M., 1998. Characterization of African swine fever virion proteins j5R and j13L: immunolocalization in virus particles and assembly sites. J. Gen. Virol. 79 (Pt. 5), 1179–1188.

Brun, A., Rodriguez, F., Parra, F., Sobrino, F., Escribano, J.M., 1999. Design and construction of African swine fever virus chimeras incorporating foreign viral epitopes. Arch. Virol. 144, 1287–1298.

Carrascosa, A.L., del Val, M., Santaren, J.F., Viñuela, E., 1985. Purification and properties of African swine fever virus. J. Virol. 54, 337–344.

Carter, G.C., Rodger, G., Murphy, B.J., Law, M., Krauss, O., Hollinshead, M., Smith, G.L., 2003. Vaccinia virus cores are transported on microtubules. J. Gen. Virol. 84, 2443–2458.

Carvalho, Z.G., De Matos, A.P., Rodrigues-Pousada, C., 1988. Association of African swine fever virus with the cytoskeleton. Virus Res. 11, 175–192.

Cobbold, C., Wileman, T., 1998. The major structural protein of African swine fever virus, p73, is packaged into large structures, indicative of viral capsid or matrix precursors, on the endoplasmic reticulum. J. Virol. 72, 5215–5223.

de Matos, A.P., Carvalho, Z.G., 1993. African swine fever virus interaction with microtubules. Biol. Cell 78, 229–234.

Esposito, J., Condit, R., Obijeski, J., 1981. The preparation of orthopoxvirus DNA. J. Virol. Methods 2, 175–179.

Esteves, A., Marques, M.I., Costa, J.V., 1986. Two-dimensional analysis of African swine fever virus proteins and proteins induced in infected cells. Virology 152, 192–206.

Finke, S., Brzozka, K., Conzelmann, K.K., 2004. Tracking fluorescence-labeled rabies virus: enhanced green fluorescent protein-tagged phosphoprotein P supports virus gene expression and formation of infectious particles. J. Virol. 78, 12333–12343.

Garcia-Escudero, R., Andres, G., Almazan, F., Viñuela, E., 1998. Inducible gene expression from African swine fever virus recombinants: analysis of the major capsid protein p72. J. Virol. 72, 3185–3195.

Geada, M.M., Galindo, I., Lorenzo, M.M., Perdiguero, B., Blasco, R., 2001. Movements of vaccinia virus intracellular enveloped virions with GFP tagged to the F13L envelope protein. J. Gen. Virol. 82, 2747–2760.

Glotzer, J.B., Michou, A.I., Baker, A., Saltik, M., Cotten, M., 2001. Microtubule-independent motility and nuclear targeting of adenoviruses with fluorescently labeled genomes. J. Virol. 75, 2421–2434.

Gomez-Puertas, P., Rodriguez, F., Ortega, A., Oviedo, J.M., Alonso, C., Escribano, J.M., 1995. Improvement of African swine fever virus neutralization assay using recombinant viruses expressing chromogenic marker genes. J. Virol. Methods 55, 271–279.

Heath, C.M., Windsor, M., Wileman, T., 2001. Aggresomes resemble sites specialized for virus assembly. J. Cell Biol. 153, 449–455.

Hernaez, B., Diaz-Gil, G., Garcia-Gallo, M., Ignacio Quetglas, J., Rodriguez-Crespo, I., Dixon, L., Escribano, J.M., Alonso, C., 2004a. The African swine fever virus dynein-binding protein p54 induces infected cell apoptosis. FEBS Lett. 569, 224–228.

Hernaez, B., Escribano, J.M., Alonso, C., 2004b. Switching on and off the cell death cascade: African swine fever virus apoptosis regulation. Prog. Mol. Subcell. Biol. 36, 57–69.

Hollinshead, M., Rodger, G., Van Eijl, H., Law, M., Hollinshead, R., Vaux, D.J., Smith, G.L., 2001. Vaccinia virus utilizes microtubules for movement to the cell surface. J. Cell Biol. 154, 389–402.

King, S.M., 2000. The dynein microtubule motor. Biochim. Biophys. Acta 1496, 60–75.

Luby-Phelps, K., 2000. Cytoarchitecture and physical properties of cytoplasm: volume, viscosity, diffusion, intracellular surface area. Int. Rev. Cytol. 192, 189–221.

Lux, K., Goerlitz, N., Schlemminger, S., Perabo, L., Goldnau, D., Endell, J., Leike, K., Kofler, D.M., Finke, S., Hallek, M., Buning, H., 2005. Green fluorescent protein-tagged adeno-associated virus particles allow the study of cytosolic and nuclear trafficking. J. Virol. 79, 11776–11787.

McDonald, D., Vodicka, M.A., Lucero, G., Svitkina, T.M., Borisy, G.G., Emerman, M., Hope, T.J., 2002. Visualization of the intracellular behavior of HIV in living cells. J. Cell Biol. 159, 441–452.

Muller, B., Daecke, J., Fackler, O.T., Dittmar, M.T., Zentgraf, H., Krausslich, H. G., 2004. Construction and characterization of a fluorescently labeled infectious human immunodeficiency virus type 1 derivative. J. Virol. 78, 10803–10813.

Murata, T., Goshima, F., Daikoku, T., Inagaki-Ohara, K., Takakuwa, H., Kato, K., Nishiyama, Y., 2000. Mitochondrial distribution and function in herpes simplex virus-infected cells. J. Gen. Virol. 81, 401–406.

Novoa, R.R., Calderita, G., Arranz, R., Fontana, J., Granzow, H., Risco, C., 2005. Virus factories: associations of cell organelles for viral replication and morphogenesis. Biol. Cell 97, 147–172.

Nunes, J.F., Vigario, J.D., Terrinha, A.M., 1975. Ultrastructural study of African swine fever virus replication in cultures of swine bone marrow cells. Arch. Virol. 49, 59–66.

Ramiro-Ibanez, F., Ortega, A., Brun, A., Escribano, J.M., Alonso, C., 1996. Apoptosis: a mechanism of cell killing and lymphoid organ impairment during acute African swine fever virus infection. J. Gen. Virol. 77 (Pt. 9), 2209–2219.

Raux, H., Flamand, A., Blondel, D., 2000. Interaction of the rabies virus P protein with the LC8 dynein light chain. J. Virol. 74, 10212–10216.

Rodriguez, J.M., Almazan, F., Viñuela, E., Rodriguez, J.F., 1992. Genetic manipulation of African swine fever virus: construction of recombinant viruses expressing the beta-galactosidase gene. Virology 188, 67–76.

Rodriguez, F., Alcaraz, C., Eiras, A., Yanez, R.J., Rodriguez, J.M., Alonso, C., Rodriguez, J.F., Escribano, J.M., 1994. Characterization and molecular basis of heterogeneity of the African swine fever virus envelope protein p54. J. Virol. 68, 7244–7252.

Rodriguez, F., Ley, V., Gomez-Puertas, P., Garcia, R., Rodriguez, J.F., Escribano, J.M., 1996. The structural protein p54 is essential for African swine fever virus viability. Virus Res. 40, 161–167.

Rodriguez, J.M., Garcia-Escudero, R., Salas, M.L., Andres, G., 2004. African swine fever virus structural protein p54 is essential for the recruitment of envelope precursors to assembly sites. J. Virol. 78, 4299–4313.

Rojo, G., Chamorro, M., Salas, M.L., Viñuela, E., Cuezva, J.M., Salas, J., 1998. Migration of mitochondria to viral assembly sites in African swine fever virus-infected cells. J. Virol. 72, 7583–7588.

Rouiller, I., Brookes, S.M., Hyatt, A.D., Windsor, M., Wileman, T., 1998. African swine fever virus is wrapped by the endoplasmic reticulum. J. Virol. 72, 2373–2387.

Sampaio, K.L., Cavignac, Y., Stierhof, Y.D., Sinzger, C., 2005. Human cytomegalovirus labeled with green fluorescent protein for live analysis of intracellular particle movements. J. Virol. 79, 2754–2767.

Smith, G.A., Enquist, L.W., 2002. Break ins and break outs: viral interactions with the cytoskeleton of mammalian cells. Annu. Rev. Cell Dev. Biol. 18, 135–161.

Sodeik, B., Ebersold, M.W., Helenius, A., 1997. Microtubule-mediated transport of incoming herpes simplex virus 1 capsids to the nucleus. J. Cell Biol. 136, 1007–1021.

Stefanovic, S., Windsor, M., Nagata, K.I., Inagaki, M., Wileman, T., 2005. Vimentin rearrangement during African swine fever virus infection involves retrograde transport along microtubules and phosphorylation of vimentin by calcium calmodulin kinase II. J. Virol. 79, 11766–11775.

Suomalainen, M., Nakano, M.Y., Keller, S., Boucke, K., Stidwill, R.P., Greber, U.F., 1999. Microtubule-dependent plus- and minus end-directed motilities are competing processes for nuclear targeting of adenovirus. J. Cell Biol. 144, 657–672.

Ward, B.M., 2005. Visualization and characterization of the intracellular movement of vaccinia virus intracellular mature virions. J. Virol. 79, 4755–4763.

Ward, B.M., Moss, B., 2001. Visualization of intracellular movement of vaccinia virus virions containing a green fluorescent protein-B5R membrane protein chimera. J. Virol. 75, 4802–4813.